



Environmentally friendly manufacturing of grinding wheels from nonwoven abrasive waste: method and performance evaluation

Korbinian Rösch¹ · Tim Mayer² · Shashank Tumkur Karnick³

Received: 1 April 2025 / Accepted: 24 August 2025 / Published online: 5 September 2025
© The Author(s) 2025

Abstract

Abrasive pads are used in a wide range of applications. The production of these pads creates significant quantities of waste consisting of plastics combined with ceramic grits, which hinders conventional recycling methods. A Research team at the University of Stuttgart utilized this waste in a novel process for the production of grinding wheels. This approach promises to save time, energy, and money. Although we faced difficulties in handling and dosing the material, iteratively changing the mixture and pressing parameters yielded usable grinding wheels. Mixing the waste material with 15% fresh phenolic resin binder resulted in a grinding wheel with mechanical and tribological properties similar to conventional products. However, its performance remains somewhat inferior to those of traditional abrasives. In real-life application tests, it withstands a rated angular velocity higher than 12,000 revolutions per minute and creates surfaces with a roughness of approximately 1.5 μm on painted metal parts. Future work should focus on developing better pore-forming agents, since those tested thus far have not sufficiently reduced surface clogging.

Keywords Polyamide · Polyurethane · Nonwoven abrasive · Grinding wheel · Recycling

1 Introduction

Grinding is a precision manufacturing process in which an abrasive tool, typically a rotating grinding wheel or a belt composed of bonded abrasive grains, removes material from the workpiece. Unlike other common material removal techniques such as CNC milling, where a defined cutting edge removes material, grinding relies on the collective effect of countless abrasive grains. Each grain acts as a microscopic, irregular cutting point, resulting in the removal of very fine chips from the workpiece. Grinding is an essential finishing

process in every metalworking industry and many other industries [1].

Within the broad category of grinding tools, nonwoven abrasives, also referred to as abrasive pads, represent a distinct subclass. They consist of an interlinked web of fibers, referred to as a “nonwoven” and often made of nylon, as well as abrasive grits [2]. These are bonded together with a binder, often phenolic resin [3]. Their flexibility is an advantage over grinding tools with more rigid binding, as it allows the abrasive particles to contact the workpiece surface in a more even manner, avoiding deeper gashes [4]. The global market for nonwoven abrasives is valued at over USD 23 billion, with an expected growth to USD 32 billion by 2030 [5].

The production of nonwoven abrasive pads generates a substantial amount of plastic waste, which has become a growing concern owing to the plastic waste crisis [6]. Awareness of the issue is growing within the abrasives industry, particularly regarding its impact on their product’s carbon footprint [7]. In response to increasing public and regulatory pressure, manufacturers are seeking ways to reduce their plastic waste output. However, waste from abrasive production is considered challenging to recycle because it contains both organic and inorganic materials in a firm bond [8]. Therefore, many contemporary recycling

✉ Korbinian Rösch
korbinian.roesch@iff.uni-stuttgart.de

¹ Institute of Industrial Manufacturing and Management IFF, University of Stuttgart, Nobelstraße 12, 70569 Stuttgart, Germany

² Fraunhofer IPA, Fraunhofer Institute for Manufacturing Engineering and Automation Nobelstraße 12, 70569 Stuttgart, Germany

³ Faculty of Process and Systems Engineering, Otto von Guericke University, Universitätsplatz 2, 39106 Magdeburg, Germany

technologies are simple downcycling, where the waste material is incorporated as filler material in e.g. mortar in cement [9].

Dissolving this bond is possible only through the use of aggressive chemicals like in [10] and [11], raising health, regulatory, and cost concerns. Therefore, many recycling techniques focus on recovering only the more expensive grit materials. For example in [12], Sabarinathan et al. used recycled grain from the milling of the stumps of used grinding wheels. Similar techniques were used in [13] to recycle abrasive grits in water jet machining. Meanwhile, in [14], Giani et al. describe a process for reclaiming abrasive particles from production waste of bound abrasives by pyrolysis, where the organic binder part is combusted.

In summary, the predominant approach releases the abrasive grits from the binder through either chemical treatment or high-temperature processes such as pyrolysis. These techniques inevitably lead to the loss of the less valuable plastic fraction and impose additional costs, including CO₂-certificates and fuel for pyrolysis [15].

Therefore, a novel method that enables the recycling or reuse of both the binder as well as the abrasive grits is needed. This approach addresses the environmental concerns associated with the burning of plastic waste and also maximizes resource efficiency. As such, it assists the industry at a time where both regulatory pressure and consumer demands lead to increased attention towards sustainability [7].

In a typical process for the production of grinding wheels, abrasive grits are first mixed with a binder and other additives in a large blender. The resulting mass is then pressed in a heated form [16]. While the initial pressing is usually completed within minutes, the uncured discs are then hardened in an oven. This final curing of the binder can take as much as 24 h, depending on the binder used and wheel thickness [17]. This step accounts for a large proportion of the time and energy use associated with the production of the grinding wheel.

However, a grinding wheel made from nonwoven abrasive waste does not require this final curing step, as no or very little uncured binder is added to the mixture. Therefore, it is much faster and more energy efficient to produce. The challenge lies in achieving sufficient cohesion in the wheel so that it can withstand the centrifugal and lateral forces during grinding. Equally important is the surface finish that is achievable with the wheel, which depends on factors such as the wheel's self-sharpening capacity, porosity, and abrasive grit. Another crucial aspect is the grinding wheel's staying power, expressed as G-Ratio, or the ratio between the workpiece wear and wheel wear [17]. If the wheels are markedly behind commercially available wheels in any of these categories, their introduction into the market will be hampered. The results are shown in Fig. 1.



Fig. 1 Bottom: Abrasive pad; Left: Recycling material; Right: Grinding disk

2 Materials and methods

2.1 Analysis of materials

Recycling material (see Fig. 2a) was provided by our project partner, a medium-sized manufacturer of abrasive pads. After the individual pads are punched out from the nonwoven abrasive roll, they are assembled and dressed on a lathe, generating small flakes of nonwoven fibers with bonded abrasives. These flakes constitute the bulk of the waste material. We began by analyzing the material provided by the project partner and determined via IR spectroscopy that its organic components are primarily made up of polyamide (PA-6,6, Nylon) and polyurethane (PU, see Fig. 2b). As expected, the particles consisted mainly of individual fibers with attached abrasive grits, which were held together by the resin.

Particle size distribution was determined by sieving. The recycled material showed a broad particle distribution between above 1 mm and below 50 μm , with a peak at 500 μm (see Fig. 3a). We then used pyrolysis to burn the organic parts, obtaining solid ceramic particles, which were studied under a microscope, as depicted in Fig. 3b. This allowed us to conclude that the majority of the abrasive particles were between 30 and 300 μm in size, with a mean of 96 μm and a standard deviation of 60 μm . This is a comparatively broad spread of grit sizes and cannot be sold as commercial recycled abrasive grits. An optical comparison between individual grits separated from the fibers showed that the abrasive grits consisted of both corundum (Al₂O₃) and silicon carbide (SiC). Again, such a mixture of softer and harder abrasives would make the abrasive grits undesirable for conventional recycling. By weighing before and after pyrolysis, we were able to determine that the grits accounted for approximately 25% of the mass of the recycled material.

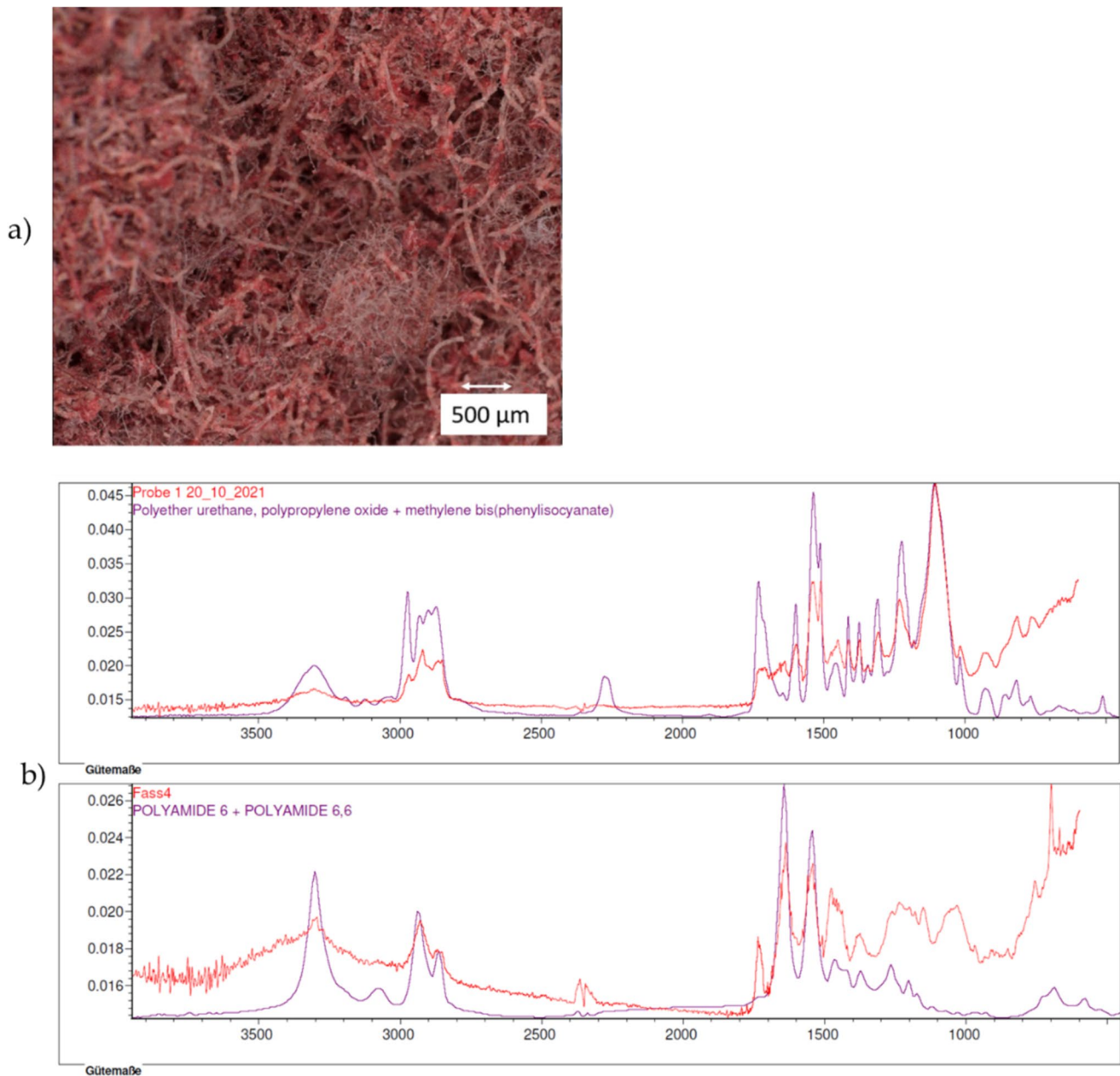


Fig. 2 (a) Raw materials as delivered; (b) result of IR-spectroscopy

2.2 Different possible approaches to recycling

Our primary focus in this project was to create a product that could absorb the waste stream of the nonwoven abrasive pad production process and innovate a superior abrasive. A cheaper price owing to the lower cost of primary materials would offset efficiency losses in grinding against conventional products, to a degree. After the analysis, several recycling methods were discussed and compared.

After investigating the average flake size, our first idea of recycling the fibers by feeding them back into a carding machine to create new rolls of nonwoven abrasive was

discarded. Despite the fact that some machines can work with shorter fibers, the average length and shape of the flakes in the recycled material are not suitable for the carding process.

Another approach that was explored involved pressing the flakes onto paper backing to produce sandpaper. However, after several attempts (see Fig. 4a), it became evident that the paper backing could not withstand flexing, as in traditional sandpaper. In test applications, the abrasion rate was much lower than that of traditional sandpaper, probably because its surface lacks the normal porosity. Moreover, the low cost of sandpaper in the market

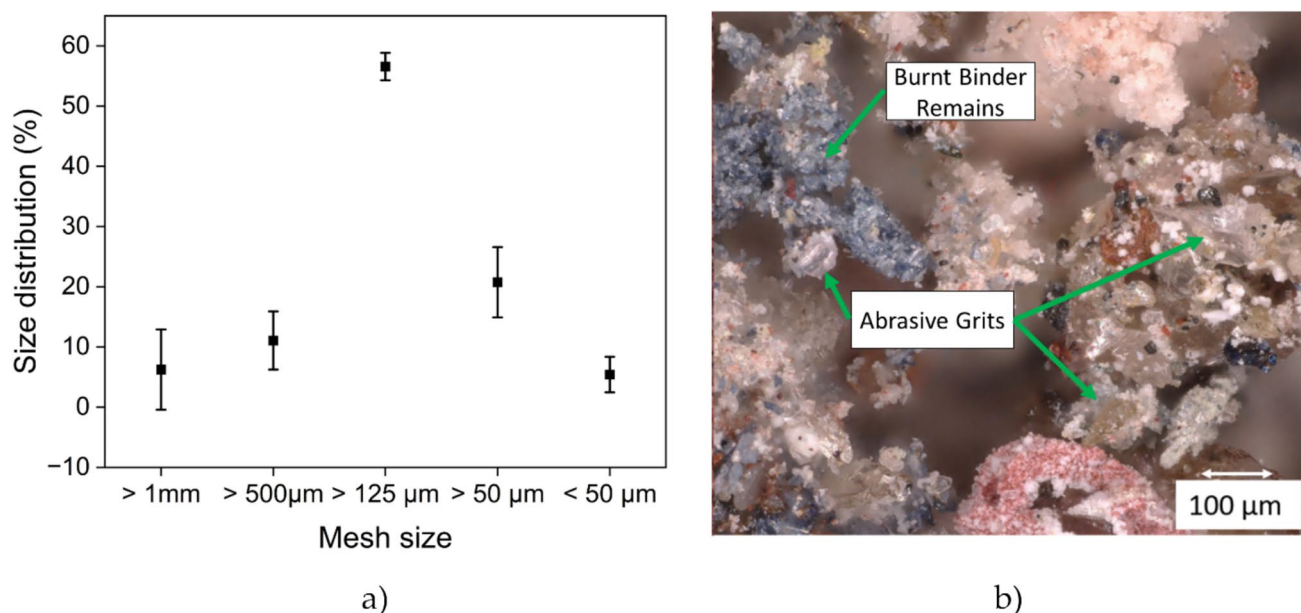


Fig. 3 (a) Size distribution determined by sieving, (b) waste material after pyrolysis

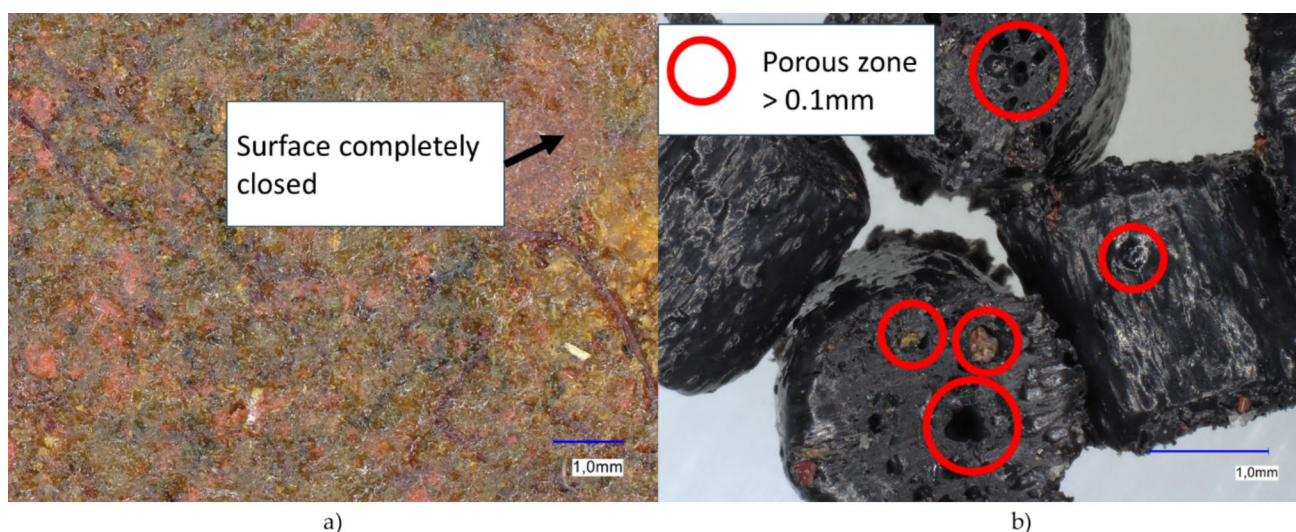


Fig. 4 (a) Sandpaper under microscope, showing the closed surface; (b) extruded granulate with marked pores

poses a significant challenge for any new product to be competitive.

A further suggestion was to utilize the waste material in the fabrication of bristles for technical brushes with embedded abrasives. It was thought that the abrasive parts could have a beneficial impact on cleaning performance. Initial trials using plastic extruders revealed that a high content of non-nylon material resulted in the formation of large pores in the extruded granulate. A microscopic image of the produced granulate is shown in Fig. 4b. This and the high content of unmeltable material made it unsuitable

for the highly precise melt-spinning process required for the creation of technical brushes. Attempts were made to stretch the filaments produced in the extrusion tests to produce bristles directly. Despite using low drawing speeds of only 5 mm/min, the filament tore at an elongation of only 9% and a load below 120 N. This unexpectedly low performance of the PA-based filament was attributed to the porosity and the presence of non-nylon materials in the extrusion. Based on these results, the idea of using waste material in the fabrication of bristles must also be abandoned.

As a result, the only idea that merited further examination and experimentation was the recycling of waste material into grinding wheels using the hot-pressing method.

2.3 Hot-pressing of grinding wheels

Before pressing, the waste material was homogenized to achieve a consistent particle size distribution, which was important for the dosing process. Specifically, the collected waste was first sieved to separate out pieces larger than 1 mm in diameter. These larger pieces were then fed through an industrial shredder until their size was reduced to below 1 mm. The shredded material was then mixed back into the powder fraction that had passed through the sieve. Finally, the entire batch was thoroughly blended using a 3D mixer to prevent the heavier abrasive grits from settling and to ensure an even distribution of abrasives throughout the mixture. No steps were taken to increase the abrasive content, such as removing binder material, to maximize the amount of material that can be recycled.

For this grinding wheel production process, a mold was designed for press heating (see Fig. 5), which was filled with powder. The grinding wheel size was set to 120 mm, which is a common size in the market. A 30-mm opening was specified at the center of the mold for CNC machine mounting, which was created via a steel stud in the mold. However, precise dosing of the material proved to be a challenge because of the agglomeration of the particles that adhered to one another.

Because there are no standard procedures for the handling and recycling of this material mix, an iterative approach to the experimental design was utilized. After initial trials, three rounds of experiments were conducted and analyzed. The results from each stage were used to decide the parameters for the subsequent experimental stage. The tests conducted at each stage were adapted as the produced wheels approached the performance of commercially available ones. Table 1 summarizes the testing process, listing the controlled factors and the measurements taken.

2.3.1 Experiment stage 0: initial trials

The goal of this stage was to familiarize ourselves with the material. No formal experimental design was utilized. These initial trials established that during the pressing process, temperatures below 120 °C and pressures below 100 kN are not sufficient to produce grinding wheels with enough toughness to remain undamaged when wheels are removed from the mold. This was only achieved at temperatures starting at 150 °C, where the wheels remained intact during demoulding. Further examination of the products was not performed. Instead, the results were used to determine the parameters for the subsequent stages of the trials.

2.3.2 Experiment stage 1: full-factorial tests without additions

Considering the materials used, an upper limit of 200 °C was set for the pressing temperature to prevent potential

Fig. 5 Press form made of the stamp and the mould

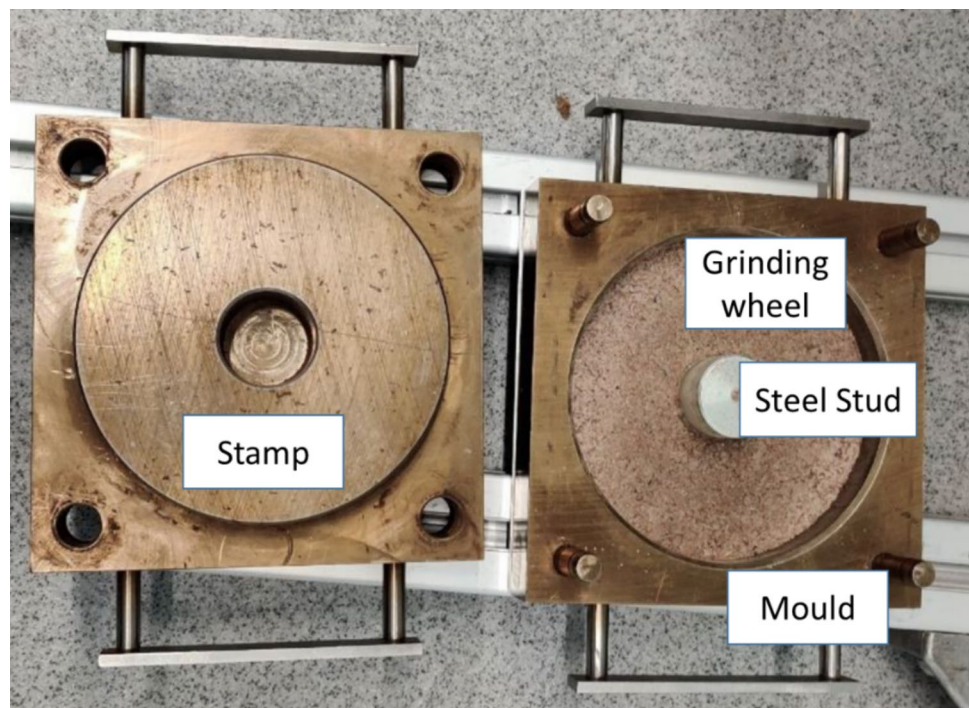
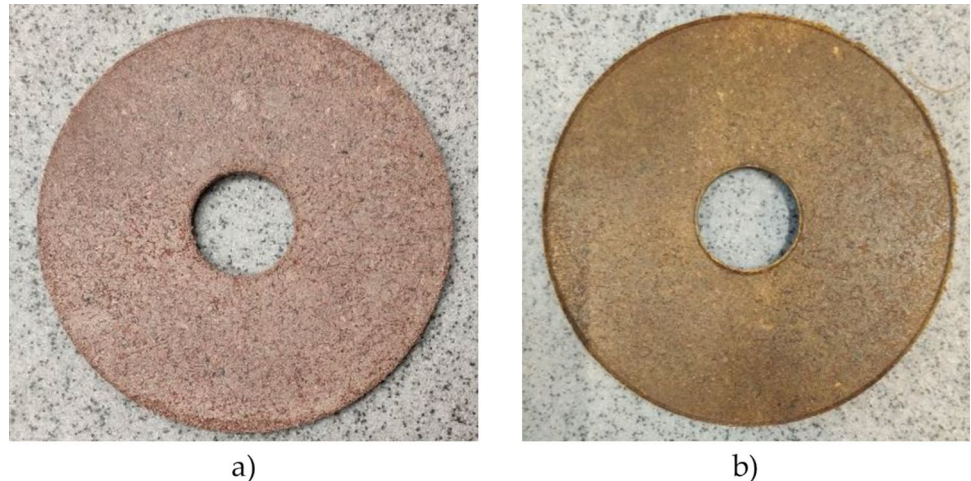


Table 1 Overview of the experimental process

Stage	Experiment type	Variables investigated	Range of variables	Measurement types
0	Initial trials	Pressure, Temperature	Pressure: 10–100 kN, 8 steps Temp: 20–120 °C	Visual: Can the grinding wheel be removed without breaking apart?
1	Full-factorial tests	Pressure, Temperature, Oven-drying; “Type A” wheels	Pressure: 100/150 kN Temp: 160/200 °C Dried: Yes/No	Tensile test, 3-Point bending test, Spin test
2	Single-Factor tests	Resin Binder content; “Type B” wheels	5/10/15/25/50% Binder	Tensile test, 3-point bending test, spin test, grinding test
3	A/B Testing	Pore forming agent, “Type C” Wheels	Agent added, Pressure 6 kN/20 kN	Spin test, grinding test

Fig. 6 (a) Type A grinding wheel without added binder; (b) Type B grinding wheel with added binder**Table 2** Factors in the Stage 1 Full-Factorial DoE plan

Temperature [°C]	Pressure [kN]	Oven-dried
160/200	100/150	Yes/no

degradation of polyurethane. To further investigate the optimal parameters, a full-factorial study was planned utilizing Design of Experiments (DoE). The study involved varying the pressing force from 100 to 150 kN and the temperature from 160 °C to 200 °C, with three specimens produced from each combination. Furthermore, we investigated if drying the material could increase its cohesion. Recycling powder as delivered was compared to the dried powder. Drying was carried out in an oven at 80 °C for 6 h. Initially, a compressed air-drying process was attempted, but clogs in the air filters made this approach unviable. Moisture content determination, performed on a MT-HX204 via the loss-on-drying method, showed that the oven drying procedure lowered the moisture content from 0.85 wt-% to 0.18 wt-% [18]. The grinding wheels produced in this section were termed “Type A” wheels. An example is shown in Fig. 6a. Table 2 summarizes the parameters of the experiment.

Subsequently, the different grinding wheel samples were subjected to mechanical testing, as described in Sect. 2.4.

The results of the mechanical tests showed that the specimens had low tensile strength. As the tensile strength is crucial for achieving a high rated velocity, it was decided that the wheels needed to be reinforced for successful application.

2.3.3 Experiment stage 2: single-factor tests with added resin binder

To enhance the mechanical performance of the grinding wheels, we added a fresh phenolic resin binder, which is also used in nonrecycled grinding wheels. An example of the wheel produced in this study is shown in Fig. 6b. We employed a full-factorial test design to systematically explore the effects of varying the binder content. Although adding uncured resin reduced the cost-saving benefit, it was considered a necessary tradeoff to ensure the production of a wheel capable of safely performing its intended tasks. The proportion of fresh binder was adjusted in 5% steps, going from 5 to 25%. A 50% mixture was attempted once, but it failed to fully cure within the designated timeframe. Based on the previous stage, in which the grinding wheels exhibited optimal mechanical properties at 160 °C, this temperature was selected for the pressing process. Mixing was performed in a Biomation Manual 3D Mixer for 3 min.

These samples, termed “Type B wheels”, were subjected to the same mechanical testing procedures for evaluation as the non-reinforced samples of Type A. When these showed sufficient quality, grinding tests were conducted, as detailed in Sect. 2.4. This revealed a need for higher porosity, as the grinding edges of the wheels were prone to clogging, leading to Experiment Stage 3.

2.3.4 Experiment stage 3: A/B testing with pore forming agent

To increase the surface porosity of the grinding wheels, a pore-forming agent was added to the mixture before mixing. TRACEL® NCS 175 was chosen as the pore-forming agent because of its use in other rubber-bound grinding wheels. As per the manufacturer’s instructions, it was added to the mixture for the wheel at a weight ratio of 1%. Mixing with the recycled material and the established 15% of fresh phenolic resin binder was carried out with the same parameters as in the previous step. A temperature of 160 °C was maintained, but it soon became apparent that the pressing force had to be lowered for the pore-forming agent to be effective. At 100 kN, the porosity, as measured via focus variation microscopy, did not differ between wheels with and without the pore former. At 20 kN, a porosity of approximately 25% was achieved, and with 6 kN, it could be increased to 30%. These two variants of grinding wheels were then evaluated via an abbreviated mechanical testing procedure, and, when they proved safe for handling, via grinding tests. For brevity, these wheels are referred to as “Type C” wheels.

2.4 Testing methods

2.4.1 Tensile and 3-point-bending tests

The specimens were cut from the Type A and B grinding wheels using a diamond wire saw according to ISO 20753. Each grinding wheel yielded three specimens, which were

taken from a distance of 30 mm from the center of the wheel. Flexural and tensile strength σ [MPa] are calculated via

$$\sigma = \frac{F}{A}, \quad (1)$$

where F is the maximal force that the piece can withstand before breaking, and A the area of its cross-section. During tensile testing, the specimen was pulled apart to apply the force, whereas in the bending test, the specimen was placed on two supports, and a punch exerted force in the middle of the specimen. Both tensile and flexural strengths were determined on a Zwick-Roell Retro-Line 20kN universal testing machine with a movement speed of 5 mm/min [19–22].

2.4.2 Spin testing

In order to ensure the safety of the grinding wheels at typical grinding speeds, spin testing was conducted on Type A, B, and C wheels. During the spin testing, the wheels were fixed on a rotating motor shaft inside an enclosure rated for ballistic testing, as shown in Fig. 7. The speed of the motor shaft increased gradually until the wheels shattered owing to the centrifugal force.

2.4.3 Grinding performance test

After ensuring the safety of the different types of grinding wheels, their grinding performances were assessed. The machine available for this step was a Reichenbacher Eco-LT 5-Axis CNC mill. Figure 8 left shows the grinding process. Owing to the wide distribution of abrasive grits, these recycling wheels are not suitable for precision surface-finishing applications. Instead, we evaluated their effectiveness in stripping paint from lacquered metal parts, which represents a typical operation where these grinding wheels are expected to be valuable.

Table 3 summarizes the experimental trial sets (hereafter referred to as “Trial Set #”), listing the types of grinding wheels tested alongside the associated test conditions,

Fig. 7 Spin testing setup; (a) Grinding wheel on spindle with standoff; (b) Top cover installed; (c) After spin testing. From [13]

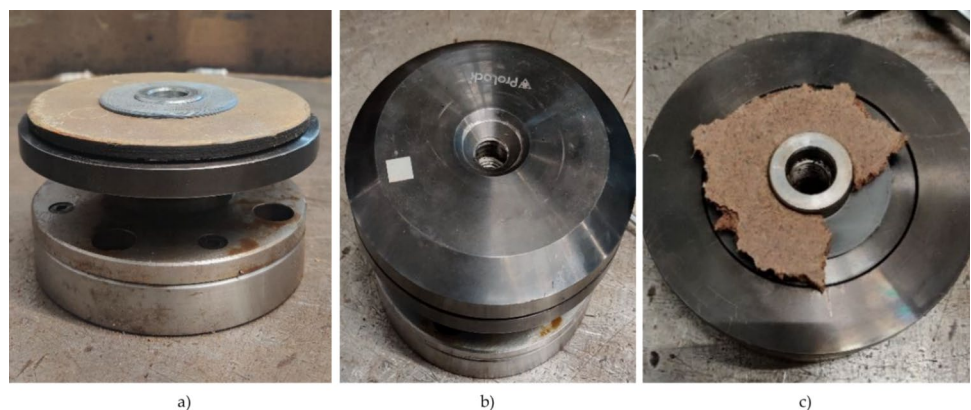


Fig. 8 (a) Grinding wheel during grinding; (b) Ground surface under light microscope, showing the grooves of different size due to different abrasive grit sizes; both from [18]

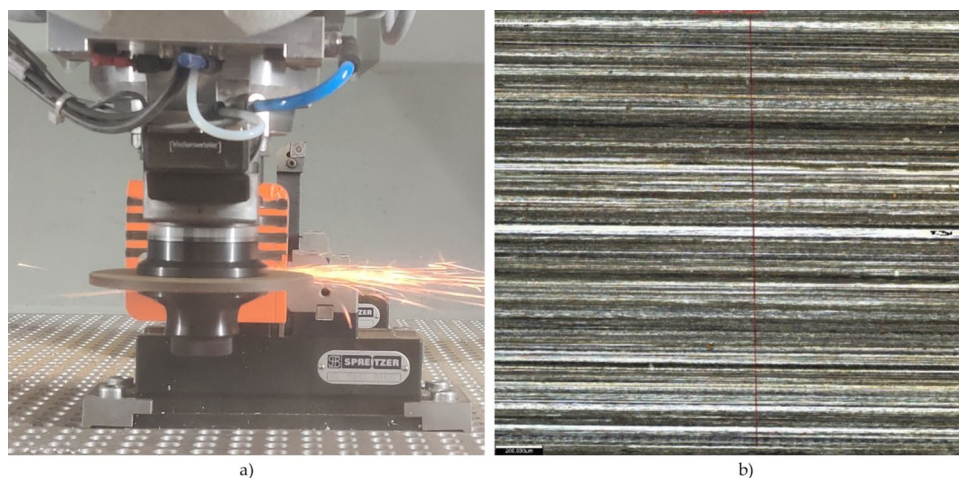


Table 3 Summary of the grinding trial sets

Trial set #	Trial phase	Type wheel	Speed (RPM)	Feed rate (mm/min)
1	(1) No Dressing	A (no binder)	2000	30
2	(1) No Dressing	A (no binder)	4000	45
3	(1) No Dressing	B (binder)	6000	30
4	(1) No Dressing	B (binder)	8000	45
5	(2) Dressing between passes	A (no binder)	2000	125
6	(2) Dressing between passes	A (no binder)	4000	250
7	(2) Dressing between passes	B (binder)	6000	125
8	(2) Dressing between passes	B (binder)	8000	250
9	(3) Evaluation of Porosity	B (binder)	4000	250
10	(3) Evaluation of Porosity	C (Pore former)	4000	250

grinding speeds, and feed rates. The grinding speed, feed rate, and infeed were selected based on real-world values for similar grinding operations; however, the results of the previous mechanical testing steps led us to limit the maximum speed for some of the weaker wheels. During the first attempt (Trial Sets #1–4), we did not dress the wheel between grinding passes, which refers to the process of restoring the cutting ability of the wheel by stripping off the outermost layer. However, the evaluation revealed significant surface clogging. To address this concern, a second trial phase was conducted in which the wheels were dressed between each grinding pass. Additionally, a higher feed rate was utilized to increase the chip thickness in an effort to reduce clogging. In Table 3, these are denoted as Trial Sets #5–8.

After finishing a grinding pass, the grinding factor G was calculated by determining the volume loss of both the grinding wheel and workpiece using the following formula:

$$G = \frac{V_w}{V_s} \quad (2)$$

where V_w is the lost wheel volume while V_s is the volume of workpiece worn away [23]. Wheel wear was assessed using digital calipers and workpiece wear by measuring the profile of the groove worn on the workpiece using a microscope. Subsequently, the surfaces generated during the grinding process were analyzed using an Alicona Infinite Focus light microscope. By employing focus variation microscopy, a 3D image of the surface was obtained, allowing the measurement of the surface roughness R_a . This is illustrated in Fig. 8b. The image shows the typical surface morphology of a part manufactured by grinding, where the abrasive grains create fine, linear parallel scratches. The red line is inserted by the user, after which the program calculates the surface roughness along that line.

To evaluate the grinding performance of the Type C wheels with additional porosity, custom test parts were created. Specifically, aluminum profiles coated with weather-proof paint were used. These components are known to be particularly prone to smearing during grinding, making them well suited to demonstrate performance differences between wheels with varying porosity. To maintain comparability with previous tests, we evaluated one grinding

wheel of Type B without additional porosity first (Trial Set #9). Subsequently, wheels with pore forming agent of Type C, pressed at both 20 kN and 6 kN, were evaluated (Trial Set #10). The grinding parameters were analogous to Trial Set #8: 4000 revolutions per minute (RPM) and a 250 mm/s feed rate. Each wheel was used for three rounds of grinding without intermediate dressing. Here, we measured two parameters: the duration of grinding before clogging became visible and the roughness of the surface before clogging.

2.4.4 Analysis of surface morphology of the grinding wheels

To complement the mechanical and application-oriented investigations described above, we also investigated the surface topography and distribution of abrasive particles in the recycled grinding wheels of Type C. This microstructural analysis offers additional context for interpreting the wheels' performance and uniformity.

First, the surface roughness of the fabricated grinding wheels was investigated using a MarSurf PS 10 tactile surface profilometer. For each grinding wheel tested, ten measurements of R_a were performed in total: five in the radial direction and five in the tangential direction relative to the wheel axis. The mean surface roughness R_a was obtained by averaging the results of all ten measurements for each wheel, providing a representative value for surface finish quality under practical grinding conditions. The locations of these measurements are shown in Fig. 9 (left).

Additionally, the spatial distribution of abrasive grits on the wheel surfaces was analyzed to verify a uniform grinding surface. We utilized optical microscopy. A representative region of each wheel was imaged with a Keyence VHX-7000

digital microscope operated at $300\times$ magnification. The acquired images were subsequently processed to identify and label abrasive particles manually, as shown in Fig. 9 (right). For quantitative assessment, the coordinates of the labeled abrasive grits were extracted and evaluated using a custom Python script. The Clark-Evans aggregation index from [24] was employed to characterize the spatial distribution of the abrasive grains, providing insight into the degree of uniformity or clustering within the abrasive-binder matrix. This algorithm is used to quantify how randomly the points are distributed in space, e.g. in quality control applications [25]. It compares the average distance between each grit and its nearest neighbor to the expected average distance, if they were randomly distributed with the same density. If the index is close to 1, this indicates a random spatial distribution. A value below 1 suggests the points are clustered in space, while a value higher than 1 indicates a more evenly spaced distribution than what would randomly occur.

3 Results

3.1 Results of mechanical and spin testing

Statistical analysis of the mechanical tests of the Stage 1 experiments with Type A wheels (without added binder) indicated that within the range of 100 to 150 kN, the pressure did not have a statistically significant impact on the maximum load attainable. This was observed in both the tensile and bending tests ($p > 0.5$). In contrast, temperature was shown to have a distinct influence ($p < 0.005$), particularly at 200 °C, where the specimens produced failed at 1/3rd of the force of those produced at 160 °C (Fig. 10).

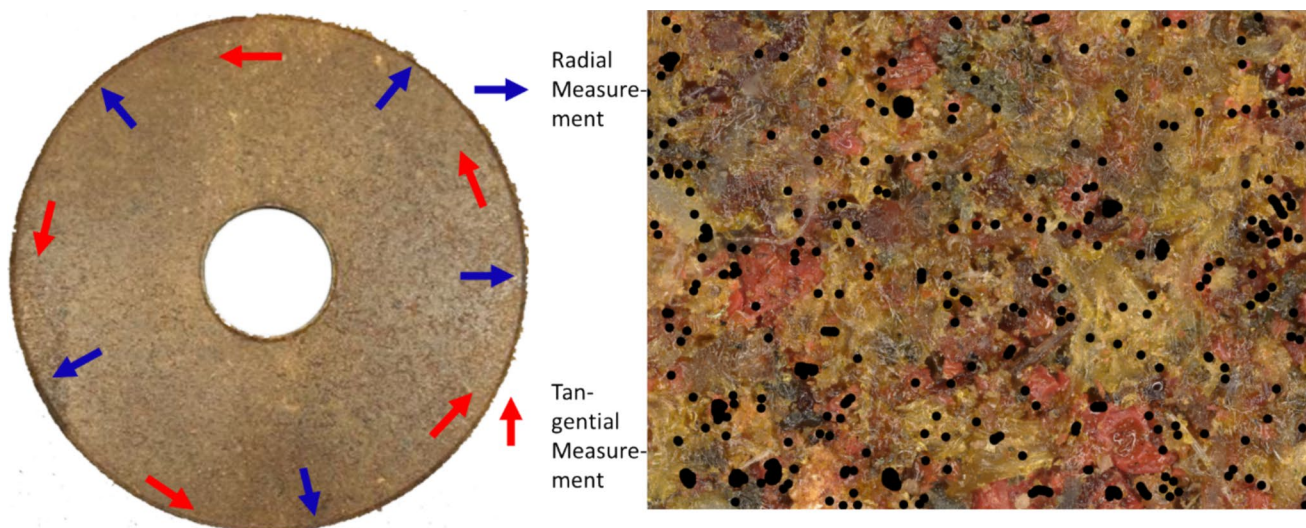


Fig. 9 Left: Locations and directions of roughness measurements; right: Microscopic surface image with locations of abrasive grits annotated

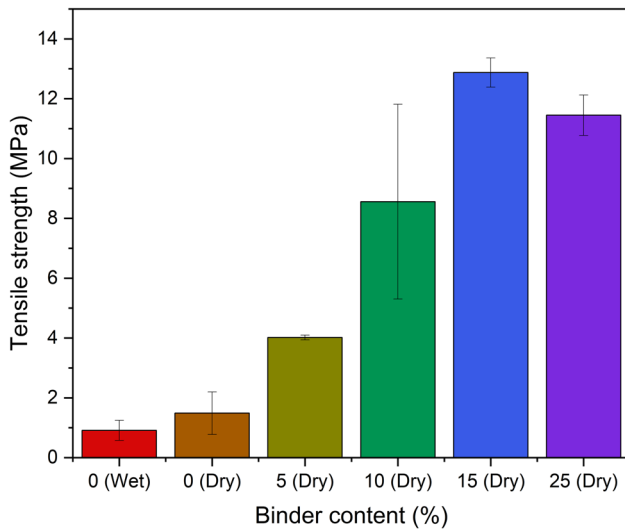
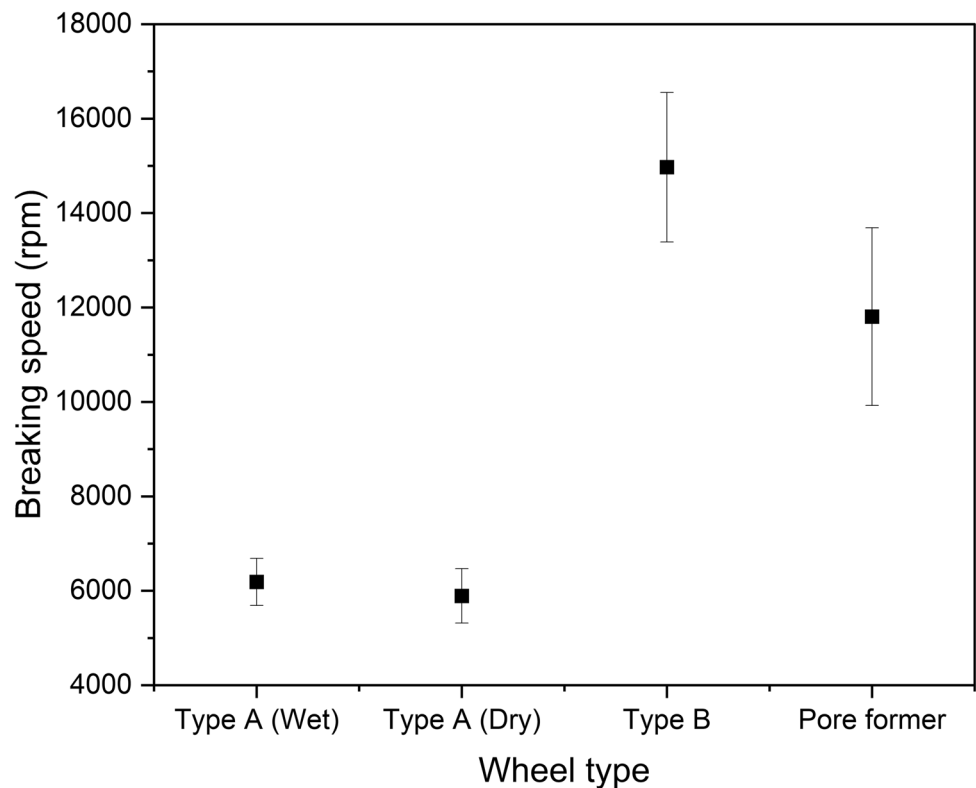


Fig. 10 Tensile strength vs binder content

This can be attributed to the thermal degradation of the PU flakes in the recycled material, leading to a decrease in their binding strength. Furthermore, it was observed that the dried specimens exhibited a significant improvement in strength compared to their non-dried counterparts ($p < 0.05$), most likely owing to the lower brittleness of the dried PA fibers compared to their non-dried counterparts.

Fig. 11 Spin testing results of different types of grinding wheel



Adding the binder significantly improved the maximum load capacity of Type B wheels, as shown in Fig. 10. Even the version with only 5% added resin created a large improvement over the Type A wheels created at the same pressure and temperature (100 kN and 160 °C). Increasing the resin percentage also increased the achievable strength, although the tensile strength was reduced at 25%. This is considered a sign of incomplete curing. Therefore, all further Type B wheels contained 15% fresh binder. Subsequently, Type C wheels were also produced with this percentage of resin.

In spin testing, Type B wheels exhibited maximum breaking speeds of approximately 14,000 RPM (see Fig. 11), similar to the performance of commercial wheels. As expected from the tensile testing results, both wheels of Type A (wet and dry) only reached a lower breaking speed, usually fracturing at or below 6000 RPM. When we repeated this test for the Type C wheels from Stage 3, their maximum speed at just below 12,000 RPM was lower than that of the Type B wheels, which can be attributed to the higher porosity reducing the effective cross section and thereby weakening the wheels' structural integrity.

As a result of these mechanical tests, all three types of wheels were used for grinding tests in enclosed machines. However, to maintain an appropriate margin of safety, it was decided to reduce the speed at which grinding with Type A wheels would be conducted compared to that with Type B wheels.

3.2 Results of grinding tests

After confirming that the wheels could withstand the mechanical stresses of normal operation, their grinding performance was evaluated. As described in Table 3, grinding tests were performed on three types of wheels (Type A dry, Type B with binder, Type C with binder and pore former) under three conditions: Trial Phase (1) without intermediate dressing, (2) with dressing between grinding passes, and (3) to test the effect of increased porosity.

During Phase (1), the grinding performance of the Type B wheels (Trial Sets 3 and 4, see Fig. 12b) produced smoother surfaces with a surface roughness R_a of less than $1.8 \mu\text{m}$, compared to the Type A wheels in Trial Sets 1 and 2, which achieved a surface roughness of $2.5 \mu\text{m}$. Additionally, as shown in Fig. 12a, the G-ratio for Type B wheels was 800,

which is significantly higher than that of Type A wheels at 200. This indicates that Type B wheels did not abrade as quickly and were more efficient in grinding operations.

However, we observed significant clogging of the grinding wheel surface owing to the low porosity of the wheels produced under high pressure. This low porosity led to frequent clogging of the grinding surfaces because the ground material could not be effectively removed, preventing new abrasive grits from being uncovered. This phenomenon affects surface quality.

Therefore, we conducted a second phase: In Phase (2), the impact of dressing the grinding wheels between passes was evaluated. Dressing significantly improved the surface roughness achieved by both the Type A and Type B wheels, see Fig. 12d. This improvement is attributed to the fact that the clogged surface impeded the self-renewing effect of the

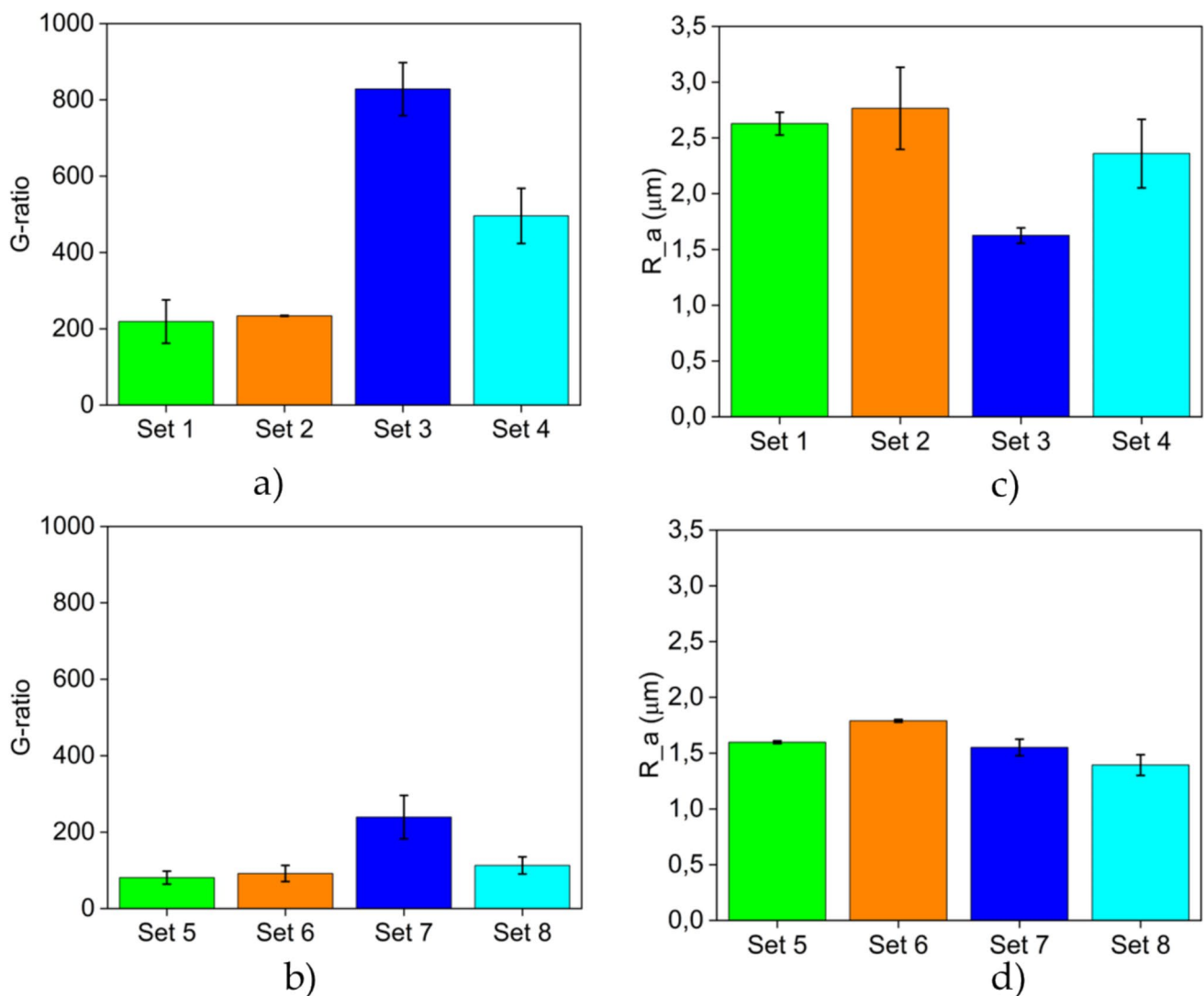


Fig. 12 (a) G-Ratio during grinding Phase 1; (b) Surface Roughness during Phase 1; (c): G-Ratio during Grinding Phase 2; (d) Surface Roughness during Phase 2

abrasive grits breaking out from the bonding. Through dressing, the surface quality improved significantly in almost all sets. Set 7, which used a Type B wheel, did exhibit a lower average R_a but showed a tighter variance. However, the dressing process also impacted the durability of the wheels as measured by their G-Value in Fig. 12c). While the Type B wheels (Trial Sets 7 and 8) were still more durable than their Type A equivalents (Trial Sets 5 and 6), their G-value sharply decreased by more than 75% due to dressing. Type A wheels were less severely impacted, losing only about 50% of their lifespan.

Since this reduction in usable lifetime due to dressing runs counter to the purpose of recycling, we designed Type C wheels to address the problem of clogging. As described in Sect. 2.4, the test used aluminum profiles lacquered in weather-proof paint. Figure 13 shows the results for these new grinding wheels (Set 10) compared with the Type B wheel (Set 9).

The pore-forming agent clearly improved the grinding length achievable before dressing was required to prevent clogging. Interestingly, the wheel pressed at 20 kN, with a porosity of only 23%, outperformed the wheel pressed at 6 kN, which had 30% porosity. Improved surface quality with higher porosity likely results from enhanced chip transport through the pores. The surface quality was worse than that in the previous grinding sets, but this value cannot be directly compared to the previous sets because the Type C wheels were evaluated on a different material. Instead, the Type C wheels of Trial Set 10 must be compared to the wheel with no pore former from Trial Set 9, which both used the same type of workpiece. Thus, the positive impact of pores becomes apparent.

3.3 Results of surface morphology analysis

As described in Sect. 2.4.4, surface roughness R_a was evaluated for the recycled grinding wheel variants of Trial Set 9 and 10. The results are shown in Fig. 14a. The sample of Type B without pore former (“No Pore Former, Set 9”) exhibited the lowest average surface roughness at $5.29 \mu\text{m}$, while the addition of a pore former (Sets 10) resulted in higher roughness values, reaching $7.21 \mu\text{m}$ at 6 kN pressure and $6.43 \mu\text{m}$ at 20 kN pressure. This indicates that the inclusion of a pore former generally increases surface roughness, likely due to enhanced porosity and a less compact wheel structure. However, increasing the pressing pressure from 6 to 20 kN partially mitigated this effect, probably due to the pores being crushed flat again.

Abrasive particle distribution was assessed from a microscope image using the Clark-Evans aggregation index, with the results displayed in Fig. 14b. The value for the wheel without pore former was 0.891, indicative of a tendency toward clustering. In contrast, the wheels containing pore former showed higher indices, 1.102 and 1.127 for 6 kN and 20 kN, respectively, demonstrating a more uniform, random distribution of abrasive particles within the matrix. These findings suggest that the addition of pore former not only affects porosity but also leads to a more homogeneous distribution of abrasive grits. Another explanation would be that the mixing of the powder containing the pore forming agent was more thorough.

In summary, the use of a pore former increased both surface roughness and perhaps the uniformity of abrasive particle distribution, while higher pressing pressure reduced roughness and enhanced uniformity further.

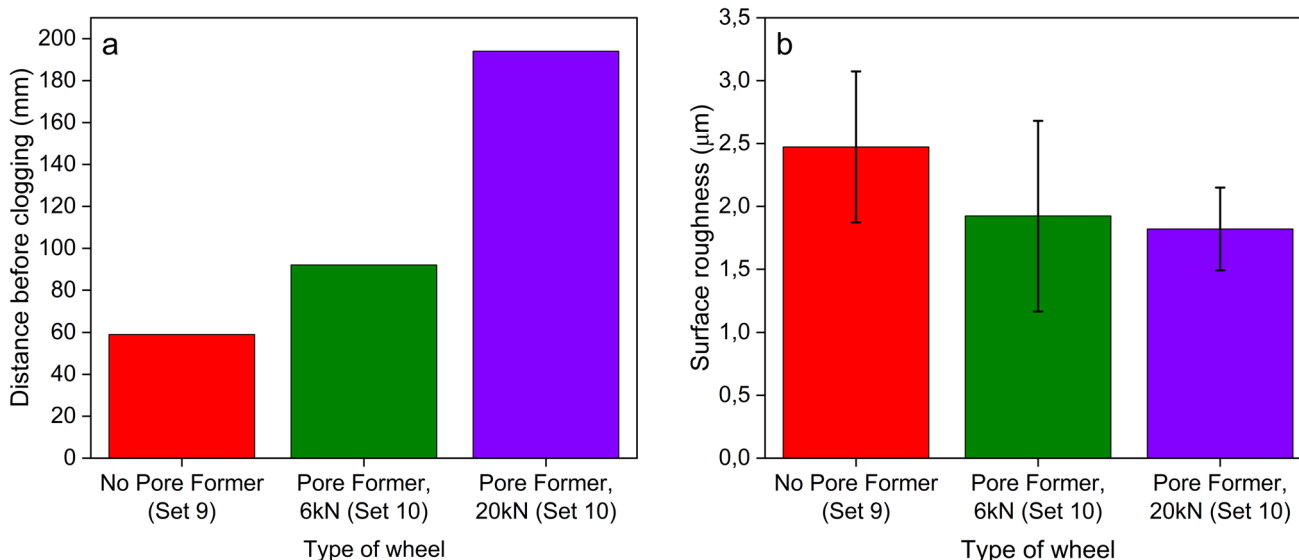


Fig. 13 (a) Distance during grinding before the wheels showed clogging of the surface; (b) Roughness of the surface before that clogging appeared

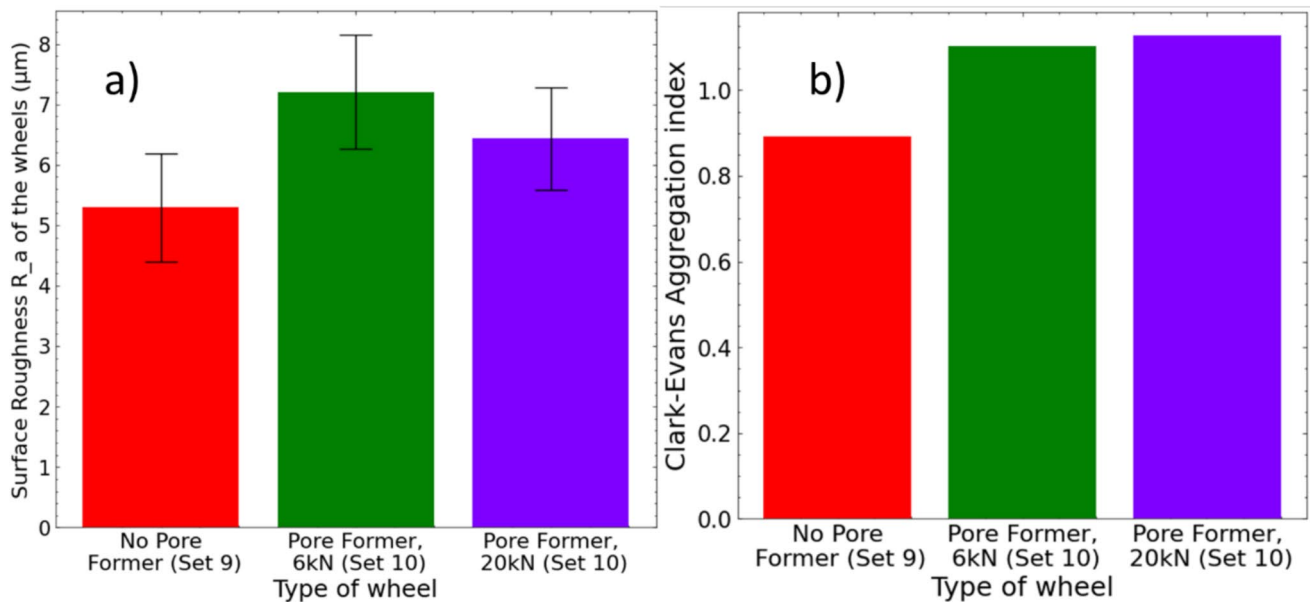


Fig. 14 (a) Surface roughness of the wheels, (b) Distribution of abrasive grits on abrasive wheels, measured by Clark-Evans Aggregation Index

These trends are clearly illustrated in the accompanying bar charts.

4 Discussion

As demonstrated in the Sect. 3, wheels made from recycled waste material can be effectively used in real-world grinding applications. A key innovation of the method presented here is the simultaneous reuse of both the thermoplastic binder and the abrasive grits from nonwoven abrasive pad waste. In contrast, most established recycling processes for grinding tool waste focus solely on recovering the valuable abrasive grains. Typically, the methods employed to separate the grains from the binder, such as chemical dissolution or pyrolysis, destroy the plastic component and result in additional emissions and waste management challenges. Meanwhile, our holistic approach reduces the need for virgin binder materials and lowers the carbon footprint of grinding wheel production.

The best surface quality was achieved with Type B wheels (15% fresh binder) at 6000 RPM and a feed rate of 125 mm/min. However, the lack of pores in the wheel leads to quick clogging of the ground material. This issue was addressed with two measures. First, frequent dressing was employed to renew the grinding surface and improve the surface quality. The drawback of this approach is a reduced service life, as the dressing process removes not only the clogged surface part but also the fresh grinding material. Therefore, we attempted to increase the porosity of the wheels by adding a 1% pore former to the mixture and lowering the pressure to

20 kN. With this new grinding wheel of Type C, the duration before clogging became apparent was increased by over 30% without compromising the quality of the ground surface. The spatial distribution of abrasive grits on these wheels was assessed quantitatively using the Clark-Evans aggregation index, revealing a very uniform dispersion of abrasive particles, as would be expected in commercial products.

It is important to note that surface quality still cannot compete with that of traditionally created grinding wheels. One reason is the broad mixture of abrasive grits stemming from the non-selective collection of production waste. Separating this waste during the production of abrasive pads via improved industrial automation and tracking could enhance the quality of the recycling wheels. Another issue is the high percentage of non-functional materials in the recycling wheels. Traditional grinding wheels also include a certain percentage of “filler material” that does not usefully interact with the workpiece, but in Type B wheels, the abrasive grits could make up as little as 20% of the final mixture of the wheel. Although the resource of abrasive waste is essentially “free,” this limits the closeness of our recycling wheel to match the capabilities of commercially available options.

Further improvements can be made by optimizing the parameters of the grinding process with these recycling grinding wheels, to account for their higher-than-usual amount of “dead weight”.

Figure 15 below is a closer investigation of the data presented in Sect. 3.2:

Generally, there is no clear relationship between speed, feed rate, and surface quality across all grinding wheels. However, for the same kind of grinding wheel, increasing

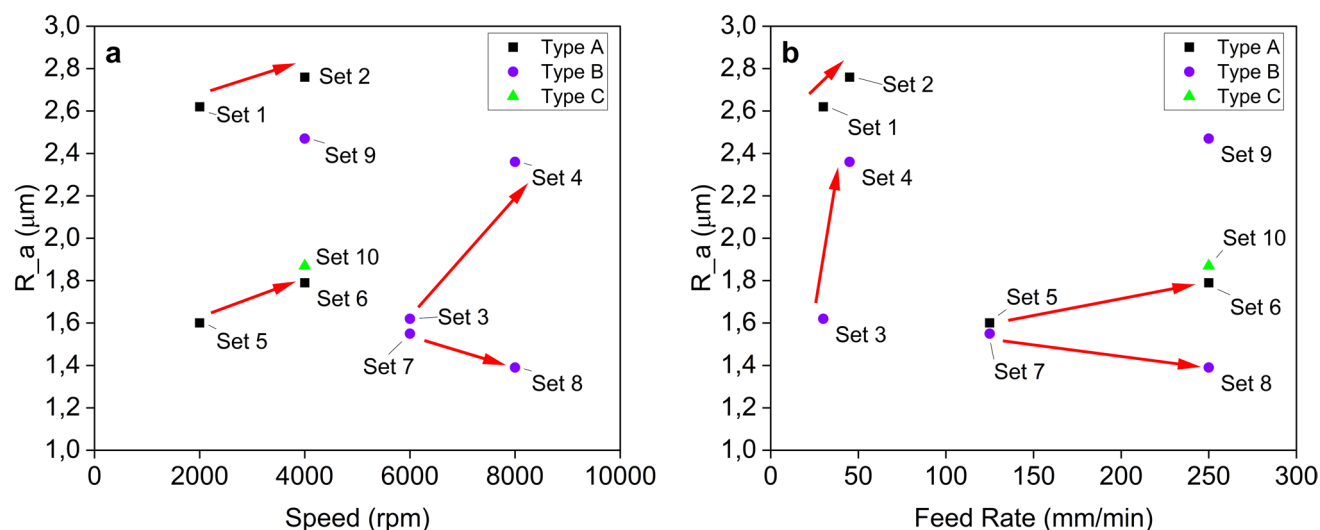


Fig. 15 Surface roughness created during the three phases of the grinding test, depending on (a) wheel speed; and (b) feed rate. Red arrows compare the same type of grinding wheel at different speed or feed rate

either the speed or the feed rate tends to increase surface roughness, resulting in lower surface quality. This relationship is shown in the figure via the red arrows. Thus, slower wheel speeds and feed rates usually yield better surfaces. The only exception to this was observed in Trial Sets 7 and 8, in which Type B wheels with intermittent dressing were used at a speed of 6000 RPM and a feed rate of 125 mm/min, and at feed rates of 8000 RPM and 250 mm/min. Here, a faster setting actually created a better surface, possibly an effect of dressing.

Nevertheless, none of the settings tested here produced surfaces acceptable for typical surface finishing applications. The uneven mixture of grain sizes and abrasive types leads to consistently irregular surfaces, making these wheels unsuitable for high-quality commercial use. Instead, we propose that these recycled grinding wheels could be used in low-quality applications where the finish on the part is not critical. Potential applications include stripping paint from metal or wood for repainting or removing rust from reclaimed metals that have been left exposed to the elements. In these low-cost applications, recycling-based grinding wheels, whose primary resource is available at no cost, will have a competitive advantage over higher-quality but more expensive products.

5 Conclusion

This study demonstrates a new approach to recycling nonwoven abrasive pad waste by enabling reuse of both the plastic binder and the abrasive grits in the production of new grinding wheels. Unlike conventional recycling technologies for abrasive products, which typically limit themselves to

recovering the grains while destroying the plastic component, our methods repurposes both parts of the waste stream. This not only reduces the reliance on virgin materials and lowers the environmental footprint of grinding wheel production but also addresses a significant gap in current recycling practices.

Despite the challenges posed by the unique properties of recycled nonwoven abrasive material, we demonstrated the feasibility of producing grinding wheels suitable for effective grinding. Although the surface quality and durability of these wheels are currently inferior to commercial products, they offer a cost-effective solution for less demanding tasks, such as surface cleaning or rust removal.

The main challenges we identified include handling and dosing of the material, as well as achieving sufficient cohesion and porosity in the final product.

Several avenues for future research are suggested. First, exploring variations in the binder and pore-forming agents used could lead to improved mechanical properties and longer service life. Second, better separation technologies for different grades of abrasives during the production of abrasive pads could enhance the quality of recycled wheels. Finally, investigating other sources of abrasive waste, such as waste from vibrational finishing, could provide a more consistent and high-quality supply of abrasive grits for recycling.

In summary, this work establishes a foundation for more sustainable, closed-loop manufacturing in the abrasives industry by demonstrating that both the binder and abrasive components of nonwoven abrasive pad waste can be effectively recycled into new grinding tools. With continued development, this approach has the potential to significantly reduce waste, conserve resources, and promote

environmentally responsible practices in abrasive tool production.

Author contribution Conceptualization, Tim Mayer; Data curation, Shashank Karnick; Formal analysis, Korbinian Rösch and Shashank Karnick; Funding acquisition, Tim Mayer; Investigation, Shashank Karnick; Methodology, Korbinian Rösch; Project administration, Korbinian Rösch; Resources, Tim Mayer; Software, Shashank Karnick; Supervision, Tim Mayer; Validation, Korbinian Rösch and Shashank Karnick; Visualization, Korbinian Rösch and Shashank Karnick; Writing—original draft, Korbinian Rösch and Shashank Karnick; Writing—review & editing, Tim Mayer.

Funding Open Access funding enabled and organized by Projekt DEAL. This research was funded by AiF GmbH as part of the Projekt Zentrale Innovationsförderung Mittelstand, grant number KK5040505AT0.

Declarations

Competing interests The authors declare no competing interests.

Open Access This article is licensed under a Creative Commons Attribution 4.0 International License, which permits use, sharing, adaptation, distribution and reproduction in any medium or format, as long as you give appropriate credit to the original author(s) and the source, provide a link to the Creative Commons licence, and indicate if changes were made. The images or other third party material in this article are included in the article's Creative Commons licence, unless indicated otherwise in a credit line to the material. If material is not included in the article's Creative Commons licence and your intended use is not permitted by statutory regulation or exceeds the permitted use, you will need to obtain permission directly from the copyright holder. To view a copy of this licence, visit <http://creativecommons.org/licenses/by/4.0/>.

References

- Klocke F, König W (2005) Schleifen, Honen, Läppen, 4., neu bearb. Aufl. VDI-Buch, / Fritz Klocke; Wilfried König; Bd. 2. Springer, Berlin
- Lukić S, Jovanić P (2004) Structural analysis of abrasive composite materials with nonwoven textile matrix. *Mater Lett* 58:439–443. [https://doi.org/10.1016/S0167-577X\(03\)00521-4](https://doi.org/10.1016/S0167-577X(03)00521-4)
- Pilato L (ed) (2010) Phenolic resins: a century of progress. Springer-Verlag, Berlin Heidelberg, Berlin, Heidelberg
- (2025) Non-woven abrasives optimize finishing while reducing grinding steps. <https://www.nortonabrasives.com/en-us/resources/expertise/non-woven-abrasives-optimize-finishing-while-reducing-grinding-steps>. Accessed 04 Jul 2025
- Research and Markets Ltd. (2025) Nonwoven abrasives market by form, end use industry, application, abrasive material, backing material, bonding, distribution channel - global forecast to 2030. <https://www.researchandmarkets.com/reports/4968583/nonwoven-abrasives-market-by-form-end-use>. Accessed 08 Jul 2025
- Linke B (2016) Life cycle and sustainability of abrasive tools. Springer International Publishing AG, Cham, RWTHedition Ser
- (2025) A strong commitment to accelerating the transition. SEAM - Sustainable European Abrasive Manufacturers
- Linke B (2016) Manufacturing and sustainability of bonding systems for grinding tools. *Prod Eng Res Devel* 10:265–276. <https://doi.org/10.1007/s11740-016-0668-5>
- Miller V (2024) Abrasive Wheel Usage | Environmental impact & sustainability. CPD Online College
- Sabarinathan P, Annamalai VE, Kumar SS et al (2019) A study on recovery of alumina grains from spent vitrified grinding wheel. *J Mater Cycles Waste Manag* 21:156–165. <https://doi.org/10.1007/s10163-018-0776-8>
- Palaniyappan S, Veiravan A, Kumar V et al (2022) Process optimization and removal of phenol formaldehyde resin coating using mechanical erosion process. *Prog Rubber Plast Recycl Technol* 38:141–154. <https://doi.org/10.1177/14777606211066316>
- Sabarinathan P, Annamalai VE, Xavier Kennedy A (2020) On the use of grains recovered from spent vitrified wheels in resinoid applications. *J Mater Cycles Waste Manag* 22:197–206. <https://doi.org/10.1007/s10163-019-00927-0>
- Sabarinathan P, Annamalai VE, Rajkumar K (2020) Sustainable application of grinding wheel waste as abrasive for abrasive water jet machining process. *J Clean Prod* 261:121225. <https://doi.org/10.1016/j.jclepro.2020.121225>
- Giani, Mario Holger et al. (2017) DE102017118017A1 - Recyclingverfahren für Schleifkörner. <https://patents.google.com/patent/DE102017118017A1/de>. Accessed 29 Mar 2023
- Eriksson O, Finnveden G (2009) Plastic waste as a fuel - CO₂-neutral or not? *Energy Environ Sci* 2:907. <https://doi.org/10.1039/B908135F>
- Marinescu ID (2013) Tribology of abrasive machining processes, 2. ed. William Andrew, Waltham, MA
- Marinescu ID, Hitchiner MP, Uhlmann E et al (2016) Handbook of machining with grinding wheels, 2nd edn. CRC Press, Boca Raton, London, New York
- Tumkur Karnick S (2023) Parameter study in the production of grinding wheels made from recycled polymer powder. Master thesis, Otto von Guericke Universität
- Deutsches Institut für Normung DIN EN ISO 527-1:2019-12, Kunststoffe_- Bestimmung der Zugeigenschaften_- Teil_1: Allgemeine Grundsätze (ISO_527-1:2019); Deutsche Fassung EN_ISO_527-1:2019
- Deutsches Institut für Normung DIN EN ISO 20753:2022, Kunststoffe - Probekörper (ISO/DIS 20753:2022): Entwurf, deutsche und englische Fassung EN ISO 20753:2022
- Deutsches Institut für Normung DIN EN ISO 527-4:2021, Kunststoffe - Bestimmung der Zugeigenschaften.
- Deutsches Institut für Normung DIN EN ISO 178:2019, Kunststoffe - Bestimmung der Biegeeigenschaften (ISO 178:2019)
- ScienceDirect (2024) Principles of modern grinding technology. <https://www.sciencedirect.com/book/9780323242714/principles-of-modern-grinding-technology>. Accessed 24 Jan 2024
- Clark PJ, Evans FC (1954) Distance to nearest neighbor as a measure of spatial relationships in populations. *Ecology* 35:445–453. <https://doi.org/10.2307/1931034>
- Scalon JD, De Silva VF, de Oliveira WA et al (2022) Statistical characterization of spatial and size distributions of particles in composite materials used in the manufacturing of biomedical instruments. *Braz J Biom* 40:428–441. <https://doi.org/10.28951/bjb.v40i4.614>

Publisher's Note Springer Nature remains neutral with regard to jurisdictional claims in published maps and institutional affiliations.